COMBINED MULTI-SCALE SIMULATIONS IN FIBER-REINFORCED COMPOSITES

F. Naya[a], C. González[a,b], C.S.Lopes[a] ,S.Van der Veen[c], J.LLorca[a,b*]

[a] *IMDEA Materials Institute, C/Eric Kandel, 2, 28906 Getafe, Madrid, Spain*
[b] *Department of Materials Science, Polytechnic University of Madrid, E.TS C.C.P., 28040 Madrid.*
[c] *AIRBUS Structures Research & Integration, ESIRNM. 18 rue Marius Terce, 31300 Toulouse, France*
**Corresponding author at: IMDEA Materials Institute, fernando.naya@imdea.org (F. Naya).*

Keywords: Multiscale, Composites, Computational Micromechanics, Nanoindentation.

Abstract

A coupled experimental-computational micromechanical framework has been developed to determine mechanical properties of a fiber-reinforced composite lamina, namely transversal compressive strength, transversal tensile strength and in-plane shear strength. This methodology includes experimental characterization of matrix and interface, combined with numerical simulations of a Representative Volume Element (RVE) of the real microstructure, reproducing fiber diameters and spatial distribution. The interface decohesion mechanism is simulated using cohesive elements. A pressure dependent, elasto-plastic model is employed to capture matrix shear yielding. Tensile and compression damage are also independently included in the matrix constitutive equation. Numerical predictions were compared with experimental results available in the literature.

1. Introduction

Carbon Fiber Reinforced Polymers (CFRP) are nowadays extensively used in applications where outstanding mechanical properties are necessary in combination with weight savings. Predicting mechanical properties and failure mechanisms in CFRP has become one of the most active areas in research activities related to material science. The influence of the microstructure and the mechanisms of deformation and fracture of the constituents in the mechanical properties of CFRP has been proven by many authors during recent years. Nevertheless, reliable and accurate failure criteria for composite materials are still under investigation. Nowadays, Computational Micromechanics has stood out as a powerful tool to predict these physical mechanisms as well as the mechanical properties, in good agreement with experimental data.

The traditional way to tackle the problem is through extensive and costly experimental programs which involve material characterization through different levels up to the final global structure. Material testing begins at the ply coupon level and a tremendous effort is needed in order to test materials under tension, compression and shear, to fully certify the different ply properties. Moreover, additional tests might be required under different ageing and environmental conditions, delaying the experimental program in months and years until final material certification.

In this work, a coupled experimental-computational micromechanical framework has been developed to determine matrix dependent mechanical properties of the composite, namely transversal compressive strength, transversal tensile strength and in-plane shear strength. This methodology includes experimental characterization of matrix and interface, combined with numerical simulations of a *Representative Volume Element* RVE.

Experimental Micromechanics is based on instrumented indentation at the fiber/matrix scale. The properties obtained at this level, the *in-situ* properties of the matrix and fiber/matrix interface, are directly used as material data for a computational micromechanics analysis. In addition, detailed information of the microstructure, such as fiber diameter distribution, volume fraction, fiber clusters and resin pockets, is captured and included in the computational model by means of a traditional RVE approach[1,2]

2. Experimental background

The material used in this work is a Carbon Fiber Reinforced Plastic (CFRP) matrix composite unidirectional laminate with aeronautical grade, obtained from Hexcel AS4/8552 prepregs. This is a well-known composite material and most of its properties can be found in the literature or are directly provided by the supplier. However, in order to validate both computational and experimental techniques presented in this work, some of them, such as matrix elastic modulus, matrix compressive strength and fiber/matrix interface strength have been estimated using the *in situ* methodology developed by Rodriguez [3,4].

2.1. Matrix nanoindentation tests

Nanoindentation tests were performed on the 8552 epoxy resin at two different environmental conditions: RT/DRY(Room Temperature; Dry atmosphere) and 70/85 (Temperature, 70 ºC; Moisture, 85%). Indentation experiments were conducted using a Hysitron TI 950 TriboIndenter equipped with a Berkovich tip (pyramidal indenter). AS4/8552 samples were previously cut using a diamond saw and polished perpendicular-to-the-fiber cross section in order to prepare them for the indentation.

Regarding matrix characterization under HOT/WET conditions, the samples were dried into a stove, AFA 200/150 Dycometal furnace, and weighted prior to be introduced in a climatic chamber, CCK-0/125 Dycometal model, at the required conditions (70/85). In order to speed up the process, the size of the samples was significantly small compared to standard travelers (manufactured according to DIN EN2823) but large enough to carry out all the instrumented indentations.

The weight of each sample was measured by means of a AG245 Mettler Toledo balance at different time intervals to check water absorption until saturation conditions were achieved (the difference between two consecutive measurement is below some specific threshold according to the EN2823 standard). At this point, several samples were taken out of the climatic chamber and used in the nanoindenter apparatus.
As the temperature of the samples fell down very fast when they were taken out of the climatic chamber, a special loading module equipped with a heating device was used instead

of the ordinary one. The tip was also a Berkovich one. Once the required temperature was reached on the surface of the sample, indentations were performed. Therefore, tests were carried out under the specific HOT/WET environmental conditions.

2.2. Fiber/Matrix interface push-in tests

In this work, the push-in technique has been chosen in order to calculate the interfacial shear strength following the methodology developed by Rodríguez [4]. All the push-in tests were performed using a *Hysitron TI 950 TriboIndenter* equipped with a 5µm diameter *flat punch* tip. According to Rodriguez [4] a 3D *finite element model* of the push-in test, taking into account real properties of the fibers and their local packing , can be used to determine the interfacial strength. The relationship obtained from the FEM model, is used to calculate the interfacial strength by means of the critical shear derived from the real *push-in* tests.

2.3. AS4/8552 fiber distribution analysis

Following the methodology developed by Vaughan[2] , the material cross section is observed and the microstructure is analyzed using an image processing program. Fibers clusters and matrix rich regions are observed. (Figure 1). Distribution of diameters and distances to the neighboring fibers are measured and fitted by statistical functions in order to generate a virtual microstructure statistically equivalent to the real one (Table 1).

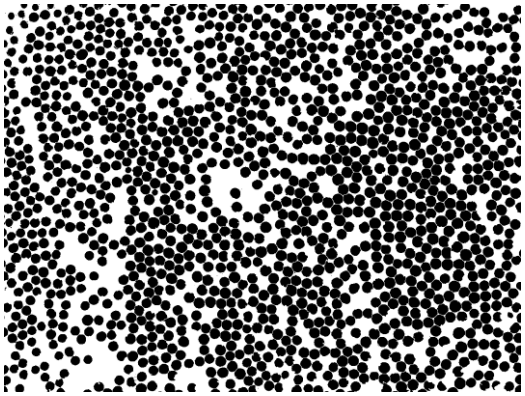

Figure 1. AS4/8552 micrograph after being processed using the *ImageJ* open source software.

Parameter	Fiber diameter[m]	1st neighbor distance[m]	2nd neighbor distance[m]
Mean	7.2476e-6	7.456936e-6	7.84089e-6
Std. deviation	0.41185e-6	0.34589e-6	0.62662e-6

Table 1. Statistical distribution parameters required to generate a virtual microstructure statistically equivalent to a real one

3. Experimental results

3.1. Matrix

The results of the indentation tests on the 8552 epoxy resin in the afore mentioned conditions (RT/DRY and 70/85) are summarized in Table 2. Regarding the Young modulus, the value obtained from nanoindentation for RT/DRY is in good agreement with the one provided by the supplier (E = 4670 MPa). Nevertheless, there is a small discrepancy between both values

that may come from two different sources, namely the estimation of the contact area and the high fiber volume fraction of the composite.

Condition	H_{ap}[Pa]	W_e/W_t	H_{ap}/σ_{yc}	β	σ_{yc} [Pa]	E [Pa]
RT/DRY	(297±30)·1e6	0.5477	1.69	29°	(176±17)·1e6	(5.07±0.3)·1e9
HOT/WET	(275±16)·1e6	0.5093	1.81	29°	(152±8)·1e6	(4.28±0.2)·1e9

Table 2. 8552 epoxy resin indentation results under RT/DRY and 70/85 conditions

3.2. Fiber/Matrix interface

A total of fifteen *push-in* tests were carried out for each environmental condition (RT/DRY and HOT/WET). The average values are gathered in Table 3. It can be observed how the interfacial strength decreases under HOT/WET conditions. Nevertheless, one consideration must be taken into account, the *push-in* tests on the conditioned samples were carried out at room temperature, so the interfacial strength can decrease even more when increasing the temperature of the test [4].

Condition	S_0 [N/m]	P_{crit} [N]	τ_{crit} [Pa]	τ_d [Pa]
RT/DRY	(105.24±2.71)·1e3	0.062495±0.003750	(30.76±1.88)·1e6	(63.77±2.64) ·1e6
HOT/WET	(119.71±7.93)·1e3	0.052261±0.003814	(29.25±1.65) 1e6	(51.58±2.72) ·1e6

Table 3. Results of AS4/8552 push-in tests under RT/DRY and HOT/WET conditions

4. Computational micromechanics

In this work, the finite element method is used to calculate the properties of the AS4/8552 composite unidirectional ply. Material properties derived using nanoindentation and push-in techniques are plugged in the constitutive equations of matrix, fiber and interface. Transverse tension strength, Y_T; transverse compression strength, Y_C, and longitudinal shear strength, S_L have been calculated using the same set of properties. Residual thermal stresses and periodic boundary conditions have been taken into account. So far, all the simulation methodology and constitutive equations have been developed using a commercial finite element software ABAQUS®/Standard. Using a Intel® Core i7-3770 CPU (3.4 GHz, 16 GB of RAM). CPU time was around one hour in all cases.

4.1. Material modeling and microstructure generation

The matrix non-linear behavior was modeled using a coupled damage-plasticity constitutive equation in order to handle the non-linearity due to plasticity in the matrix under compressive stress states and the quasi-brittle behavior under tensile loads. Among the different choices available in ABAQUS®/Standard, the *Concrete Damaged Plasticity* model stands out as one of the most suitable ones in order to represent the quasi-brittle behavior of the epoxy matrix [5].

The AS4 carbon fibers are modeled in this work as linear, elastic and transversally isotropic solids. The fiber/matrix interface is represented using ABAQUS®/Standard cohesive elements (COH3D8). The interfacial strength calculated by means of the push-in tests is introduced here. A quadratic criterion is chosen regarding damage initiation. Damage evolution is simulated using a mixed mode behavior. The *Mode I* and *Mode II* fracture

energies are set equal to the values used by Lopes [6]. The properties employed in the simulations are gathered in Table 4.

The microstructure of the composite is idealized as a dispersion of cylinders which represents the shape of the fibers. In this work two well-known algorithms, namely, the *Random Sequential Adsorption* (RSA) algorithm [1] and the *Nearest Neighbor Algorithm* (NNA)[2] were modified in order to generate a virtual three dimensional RVE (Figure 2). The fibers distribution is generated according to the information extracted from real micrographs of the AS4/8552 material (fiber radius, volume fraction, etc.).

8552 Epoxy matrix properties (RT/DRY)							
ρ[Kg/m^3]	**E[Pa]**	**ν**	**X^T[Pa]**	**β**	**σ_{yc} [Pa]**	**G_{IC}[J/m^2]**	**α[K^{-1}]**
1301	5.07e9	0.35	121e6	29^o	176e6	100	52e-6

AS4 Carbon fiber properties							
ρ[Kg/m^3]	**E_1[Pa]**	**E_2[Pa]**	**G_{12}[Pa]**	**G_{23}[Pa]**	**ν_{12} [Pa]**	**α_1[K^{-1}]**	**α_2[K^{-1}]**
1790	231e9	12.97e9	11.28e9	4.45e9	0.3	-0.63e-6	7.2e-6

AS4/8552 interface properties (RT/DRY)					
σ_1[Pa]	**τ_2[Pa]**	**τ_3[Pa]**	**G_{IC}[J/m^2]**	**G_{IIC}[J/m^2]**	**G_{IIC}[J/m^2]**
42e6	63e6	63e6	280	790	790

Table 4. Matrix, fibers and interface properties used in the simulations

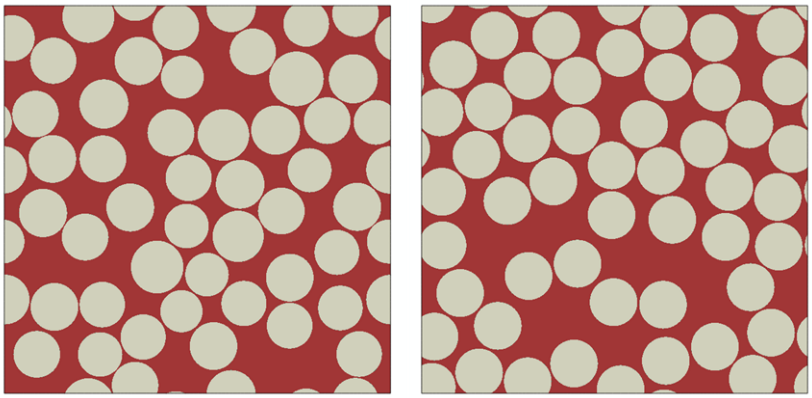

Figure 2. Virtual microstructures, generated using the NNA(left) and RSA(right) algorithms.

4.2. Transverse loading

Regarding the transverse tension (TT) loading, the main fracture mechanism is the fiber/matrix debonding, which is dominated by the interface strength and toughness. Debonding starts in those regions where the stress concentration in the fiber/matrix interface is higher (typically inside fiber clusters). After failure of the interface the matrix undergoes severe plastic deformation and "matrix ligaments" appear. While the matrix continues to accumulate plastic strain, it starts to damage, such that these ligaments cannot resist and fully developed crack appears perpendicular to the loading direction (Figure 3). A crack perpendicular to the loading axis is the predominant failure mechanisms in accordance with the experimental results. The final transverse-to-the-fiber tensile strength is determined by the interface properties as well as the spatial distribution of the fibers (clustering, etc.).

In the case of transverse compression (TC), a significant effect of hydrostatic stresses is observed. In this case, the failure mechanism corresponds to a shear band angle with respect to the loading axis (in opposition to the brittle crack perpendicular to the loading axis of the previous case). The epoxy matrix can undergo high plastic deformation before failing. As the plastic deformation progresses, debonding can be observed at the fiber/matrix interfaces in the polar regions of the fibers with respect to the loading direction (fiber poles). Similarly to the transverse tension case, debonding initiates in the highly stressed fiber cluster regions. Due to the compressive resistance of the matrix, the composite can hold a relatively high level of strain (typically around 4% or 5%). Nevertheless, as the matrix accumulates enough plastic deformation, the compressive damage mechanisms appears leading to the final fracture and failure in the microstructure (Figure 4).

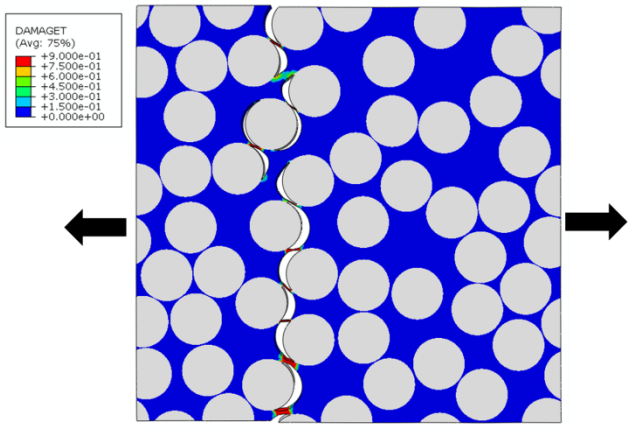

Figure 3. Matrix tensile damage in AS4/8552 under TT. Load applied in the horizontal direction.

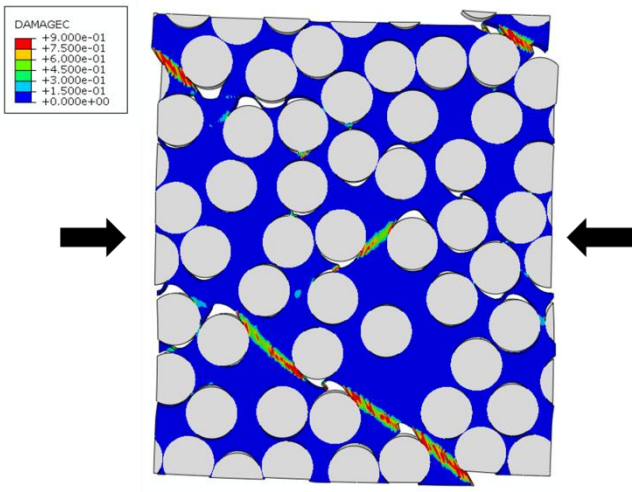

Figure 4. Matrix compression damage in AS4/8552 under TC. Load applied in the horizontal direction**.**

4.3. Shear loading

When shear loading is applied to the RVE two different behaviors are found depending on the shear direction, parallel or perpendicular to the fibers direction. If shear is applied parallel to the fibers ($\tau_{\parallel}$), according to Totry [7],the failure mechanism is dominated by interfacial decohesion which highly depends on the interface strength. The interface fracture limits the load transfer between matrix and fibers, leading to a softening after matrix yielding. In this work, the interface strength is slightly lower than the matrix shear. Fracture starts due to the

interface debonding, similar to the transverse tensile case. The cohesive interfaces fail and a crack propagates in a plane parallel to $\tau_{\parallel}$ (Figure 5, left). When the interface is totally broken, the matrix starts to hold high shear loads and a band of plastic deformation is created.

On the other hand, if shear in the plane perpendicular to the fiber is applied ($\tau_{\perp}$),the deformation pattern after matrix yielding is totally different. Once the debonding has started, matrix deformation cannot progress independently of the fibers. In order to accommodate the shear strain in the matrix, fibers start to rotate (Figure 5, right) and the composite response becomes stiffer. The in-plane shear response of the composite (τ_{12}) can be approximated as the mean value between $\tau_{\parallel}$ and $\tau_{\perp}$.

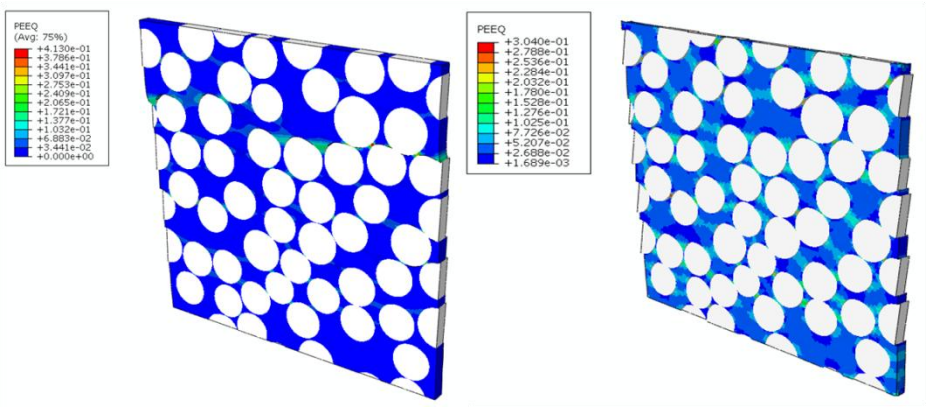

Figure 5. Plastic equivalent strain in AS4/8552: under $\boldsymbol{\tau_{\parallel}}$ just after debonding (left) and $\boldsymbol{\tau_{\perp}}$ just after the beginning of fiber rotation (right).

The predicted values of the elastic constants (transverse elastic modulus and in-plane shear modulus) as well as the transversal compressive strength, transversal tensile strength and in-plane shear strength are gathered in Table 5.

Condition	E_2[Pa]	G_{12}[Pa]	Y_T[Pa]	Y_C[Pa]	$S_L(\gamma=0.2\%)$[Pa]	$S_L(\gamma=5\%)$[Pa]
RT/DRY	9.17e9	4.83e9	72e6	277e6	55e6	88e6
HOT/WET	8.33e9	4.31e9	45e6	237e6	47e6	77e6

Table 5.Predicted elastic constants, transversal and shear strengths of a AS4/8552 lamina

5. Conclusions

In this work, transversal properties have been determined using a 3D FEM model that takes into account the real fiber distribution (fiber packing, clusters, matrix rich regions, etc. can be taken into account). All the simulations were carried out using the commercial software ABAQUS®/Standard. Neither user-defined material subroutines nor user-defined elements were used in this work. All the constitutive equations are available in the Abaqus material library. In addition, the ply strengths calculated in this work have been determined using the same set of micromechanical parameters, The model was able to reproduce the stress-strain curves (without fitting parameters), as well as the deformation and fracture mechanisms experimentally observed. In particular, the simulations of the compression tests reproduced the shear yielding of the matrix and the nucleation of the debonding, while the simulations of the tensile test showed the beginning of the damage at the interfaces and the subsequent failure of the matrix ligaments.

The work summarized in this report suggests the possibility of replacing (at least partially) the physical characterization tests by virtual ones, based on a complete characterization of the microconstituents. These virtual tests provide full control of the composite microstructure and constituent properties. Moreover, very complex stress states and parametric studies can be performed to optimize the composite properties.

References

[1] J. Segurado, J. Llorca. A numerical approximation to the elastic properties of sphere-reinforced composites. *Journal of the Mechanics and Physics of Solids*, volume (50) : 2107–2121, 2002.

[2] T.J. Vaughan, C.T. McCarthy. A combined experimental–numerical approach for generating statistically equivalent fibre distributions for high strength laminated composite materials. *Composites Science and Technology*, volume (70) : 291–297, 2010.

[3] M. Rodríguez, J.M. Molina-Aldareguía, C. González, J. LLorca. Determination of the mechanical properties of amorphous materials through instrumented nanoindentation. *Acta Materialia*, volume (60) : 3953–3964, 2012.

[4] M. Rodríguez, J.M. Molina-Aldareguía, C. González, J. LLorca. A methodology to measure the interface shear strength by means of the fiber push-in test. *Composites Science and Technology*, volume (72) : 1924–1932, 2012.

[5] L.P. Canal, J. Segurado, J. LLorca. Failure surface of epoxy-modified fiber-reinforced composites under transverse tension and out-of-plane shear. *International Journal of Solids and Structures*, volume (46) : 2265–2274, 2009.

[6] C.S. Lopes, P.P. Camanho, Z. Gürdal, P. Maimí, E.V. González. Low-velocity impact damage on dispersed stacking sequence laminates. Part II: Numerical simulations. *Composites Science and Technology*, volume (69) : 937–947, 2009.

[7] E. Totry, J.M. Molina-Aldareguía, C. González, J. LLorca. Effect of fiber, matrix and interface properties on the in-plane shear deformation of carbon-fiber reinforced composites. *Composites Science and Technology*, volume (70) : 970–980, 2010.